

Catalytic Nitrile Hydration with $[\text{Ru}(\eta^6\text{-}p\text{-cymene})\text{Cl}_2(\text{PR}_2\text{R}')]$ Complexes: Secondary Coordination Sphere Effects with Phosphine Oxide and Phosphinite Ligands

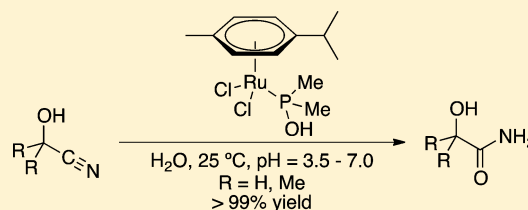
Spring Melody M. Knapp,^{†,§} Tobias J. Sherbow,[†] Robert B. Yelle,[†] J. Jerrick Juliette,[‡] and David R. Tyler^{*,†}

[†]Department of Chemistry, University of Oregon, Eugene, Oregon 97403, United States

[‡]Dow Advanced Materials-Performance Monomers, The Dow Chemical Company, Deer Park, Texas 77536, United States

Supporting Information

ABSTRACT: The rates of nitrile hydration reactions were investigated using $[\text{Ru}(\eta^6\text{-}p\text{-cymene})\text{Cl}_2(\text{PR}_2\text{R}')]$ complexes as homogeneous catalysts, where $\text{PR}_2\text{R}' = \text{PMe}_2(\text{CH}_2\text{P}(\text{O})\text{Me}_2)$, $\text{PMe}_2(\text{CH}_2\text{CH}_2\text{P}(\text{O})\text{Me}_2)$, $\text{PPh}_2(\text{CH}_2\text{P}(\text{O})\text{Ph}_2)$, $\text{PPh}_2(\text{CH}_2\text{CH}_2\text{P}(\text{O})\text{Ph}_2)$, PMe_2OH , $\text{P}(\text{OEt})_2\text{OH}$. These catalysts were studied because the rate of the nitrile-to-amide hydration reaction was hypothesized to be affected by the position of the hydrogen bond accepting group in the secondary coordination sphere of the catalyst. Experiments showed that the rate of nitrile hydration was fastest when using $[\text{Ru}(\eta^6\text{-}p\text{-cymene})\text{Cl}_2\text{PMe}_2\text{OH}]$: i.e., the catalyst with the hydrogen bond accepting group capable of forming the most stable ring in the transition state of the rate-limiting step. This catalyst is also active at pH 3.5 and at low temperatures—conditions where α -hydroxynitriles (cyanohydrins) produce less cyanide, a known poison for organometallic nitrile hydration catalysts. The $[\text{Ru}(\eta^6\text{-}p\text{-cymene})\text{Cl}_2\text{PMe}_2\text{OH}]$ catalyst completely converts the cyanohydrins glycolonitrile and lactonitrile to their corresponding α -hydroxyamides faster than previously investigated catalysts. $[\text{Ru}(\eta^6\text{-}p\text{-cymene})\text{Cl}_2\text{PMe}_2\text{OH}]$ is not, however, a good catalyst for acetone cyanohydrin hydration, because it is susceptible to cyanide poisoning. Protecting the $-\text{OH}$ group of acetone cyanohydrin was shown to be an effective way to prevent cyanide poisoning, resulting in quantitative hydration of acetone cyanohydrin acetate.



INTRODUCTION

The hydration of acetone cyanohydrin to α -hydroxyamide products is an important step in the production of acrylic monomers.¹ Acetone cyanohydrin hydration is carried out industrially using sulfuric acid, but considerable amounts of ammonium hydrogen sulfate byproduct are produced, which requires significant energy and effort to recycle.² A potentially desirable alternative process would be catalytic hydration using a homogeneous catalyst. Catalytic hydration of cyanohydrins is challenging because cyanohydrins degrade readily under basic conditions and at high temperatures to produce HCN.^{3–5} The cyanide thus produced reacts irreversibly with organometallic catalysts, poisoning the catalysts.^{6–8} Cyanohydrins can be stabilized under acidic conditions and at low temperatures, although a survey of the catalytic nitrile hydration literature shows that few nitrile hydration catalysts are functional under these conditions.⁹ For example, platinum phosphinito,⁶ molybdocene,⁶ and ruthenium^{7,8} nitrile hydration catalysts have shown limited success for cyanohydrin hydration, especially for the hydration of bulky cyanohydrins.

On paper, complete cyanohydrin hydration would be possible with a homogeneous catalyst if the catalyst was fast under conditions that stabilize the cyanohydrin—namely, low pH and low temperatures. The rate-determining step of nitrile hydration is typically attack by an external water or hydroxide

molecule on the coordinated nitrile.^{9,10} However, decreasing the pH of the solution will decrease the amount of hydroxide present in solution, potentially leading to a corresponding decrease in the rate of the hydration reaction. To increase the rate of hydration, we hypothesized that incorporation of a hydrogen bond accepting ligand in the secondary coordination sphere (e.g., Figure 1) would activate water for nitrile hydration, even under acidic conditions, meaning that these catalysts might be sufficiently fast under acidic conditions to hydrate cyanohydrins.

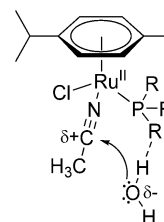


Figure 1. Proposed structure showing how hydrogen bonding of a water molecule to the secondary coordination sphere of a catalyst will activate the water molecule for nitrile hydration.

Received: May 2, 2013

Secondary coordination sphere effects in nitrile hydration reactions have been previously investigated by our group using $[\text{Ru}(\eta^6\text{-}p\text{-cymene})\text{Cl}_2\text{PR}_3]$ complexes, where $\text{R} = \text{NMe}_2$, OMe , Et .^{7,8} These studies showed that the catalyst with the best hydrogen bond accepting ligand ($\text{R} = \text{NMe}_2$) has the fastest rate of nitrile hydration. Furthermore, we showed that $[\text{Ru}(\eta^6\text{-}p\text{-cymene})\text{Cl}_2\text{P}(\text{NMe}_2)_3]$ operates by a general base catalysis mechanism, meaning that the amine functionality on the ligand does not simply act as a base and raise the concentration of hydroxide in solution.⁸ Cadierno¹¹ and Frost¹² also investigated the effect of amines in the secondary coordination sphere with similar $[\text{Ru}(\eta^6\text{-arene})\text{Cl}_2(\text{PR}_2\text{R}')] \text{-type}$ complexes. Cadierno and co-workers found that nitrile hydration reactions using the amine-containing complexes $[\text{Ru}(\eta^6\text{-arene})\text{Cl}_2\text{PPh}_2\text{R}]$, where $\text{R} = 2\text{-C}_6\text{H}_5\text{CH}_2\text{NHR}'$, $3\text{-C}_6\text{H}_5\text{CH}_2\text{NHR}'$, $4\text{-C}_6\text{H}_5\text{CH}_2\text{NHR}'$ and $\text{R}' = i\text{Pr}$, $t\text{Bu}$, were significantly faster than nitrile hydration reactions with the corresponding triphenylphosphine complex ($\text{R} = \text{Ph}$).¹¹ However, addition of 1 equiv of $\text{PhCH}_2\text{NH}i\text{Pr}$ or $\text{PhCH}_2\text{NH}t\text{Bu}$ to the $[\text{Ru}(\eta^6\text{-arene})\text{Cl}_2\text{PPh}_3]$ -catalyzed reactions increased the hydration rates to the same rates observed for the aminophosphine-containing complexes. They concluded that the rate enhancement observed was likely due to the inherently basic nature of the amine group, which would generate more hydroxide in solution.

Frost and co-workers investigated nitrile hydration with a series of β -aminophosphine-derived $[\text{Ru}(\eta^6\text{-toluene})\text{Cl}_2\text{PR}_3]$ complexes, where $\text{PR}_3 = \text{PTA-CHPhNHPH}$, $\text{PTA-CH}(p\text{-C}_6\text{H}_4\text{OCH}_3)\text{NHPH}$, $\text{PTA-CPh}_2\text{NHPH}$. Nitrile hydration with these complexes was slightly faster than that with the parent $[\text{Ru}(\eta^6\text{-toluene})\text{Cl}_2\text{PTA}]$ catalyst.¹² These complexes did not show the expected enhanced activity that had previously been observed for nitrile hydration catalysts containing amine groups in the secondary coordination sphere. The explanation was shown to be that the $[\text{Ru}(\eta^6\text{-toluene})\text{Cl}_2\text{PR}_3]$ catalysts are hemilabile. The amine group can therefore bond to the Ru center; this prevents nitrile coordination and thereby decreases the catalyst activity.

These results suggest there may be a limit to the distance from the active site where a hydrogen bond accepting group can be placed in order to increase the rate of nitrile hydration. We decided, therefore, to investigate the effect of the hydrogen bond accepting group position on the rate of hydration. In order to limit any possibility of the catalyst acting as a base (as was seen with the amine-containing ligands used by Cadierno¹¹) or coordination of the hydrogen bond accepting group (as was seen with the amine-containing ligands used by Frost¹²), a different hydrogen bond accepting group was used: namely, phosphine oxides. Phosphine oxides are some of the strongest hydrogen bond accepting groups, with an average $\text{R}_3\text{P}=\text{O}\cdots\text{H}-\text{OH}$ hydrogen bond length of 1.846(4) Å (in comparison to a trialkylamine and a dialkyl ether with average donor $\cdots\text{H}-\text{OH}$ distances of 1.96(1) and 1.978(9) Å, respectively).¹³ To investigate the effect of hydrogen bond accepting group position on the rate of hydration, the $[\text{Ru}(\eta^6\text{-}p\text{-cymene})\text{Cl}_2(\text{PR}_2\text{R}')] \text{-type}$ complexes were synthesized, where $\text{PR}_2\text{R}' = \text{Ph}_2\text{P}(\text{CH}_2\text{P}(\text{O})\text{Ph}_2)$ (dppmO), $\text{Me}_2\text{P}(\text{CH}_2\text{P}(\text{O})\text{Me}_2)$ (dmpmO), $\text{Ph}_2\text{P}(\text{CH}_2\text{CH}_2\text{P}(\text{O})\text{Ph}_2)$ (dppeO), $\text{Me}_2\text{P}(\text{CH}_2\text{CH}_2\text{P}(\text{O})\text{Me}_2)$ (dmpeO), $\text{Me}_2\text{P}(\text{OH})$, $(\text{EtO})_2\text{P}(\text{OH})$. The results of our study are reported herein.

EXPERIMENTAL SECTION

Materials and Methods. Unless stated otherwise, all manipulations were carried out in either an N_2 -filled Vacuum Atmospheres

Co. glovebox or on a Schlenk line using N_2 . HPLC grade THF, dichloromethane, hexanes, acetonitrile, and diethyl ether (Burdick and Jackson) were dried and deoxygenated by passing them through commercial columns of CuO, followed by alumina, under an argon atmosphere. HPLC grade water was degassed by sparging with N_2 . Chloroform was distilled under N_2 from CaH_2 and degassed by three freeze–pump–thaw cycles. Petroleum ether (35–60 °C; Mackron Chemicals) was degassed by three freeze–pump–thaw cycles. $[\text{RuCl}_2(\eta^6\text{-}p\text{-cymene})]_2$, 1,2-bis(diphenylphosphino)methane monoxide (dppmO), 1,2-bis(diphenylphosphino)ethane monoxide (dppeO), 1,2-bis(dimethylphosphino)methane, and 1,2-bis(dimethylphosphino)ethane were obtained from Strem. Acetone cyanohydrin, lactonitrile, and glycolonitrile (55 wt % in H_2O) were obtained from Sigma Aldrich. Cyanohydrins were distilled prior to use. All other commercially available reagents were used as received. $[\text{Ru}(\eta^6\text{-}p\text{-cymene})\text{Cl}_2(\text{dppeO})]$,¹⁴ $[\text{Ru}(\eta^6\text{-}p\text{-cymene})\text{Cl}_2(\text{dppmO})]$,¹⁴ $[\text{Ru}(\eta^6\text{-}p\text{-cymene})\text{Cl}_2\text{P}(\text{NMe}_2)_3]$,¹⁵ dimethylphosphine oxide,¹⁶ diethylphosphinate,¹⁷ and 2-acetoxy-2-methylpropanenitrile¹⁸ were synthesized following literature procedures. The ligands 1,2-bis(dimethylphosphino)methane monoxide (dmpmO) and 1,2-bis(dimethylphosphino)ethane monoxide (dmpeO) were synthesized following a modified literature procedure¹⁹ as described in the Supporting Information.

Instrumentation. Nuclear magnetic resonance spectra were recorded on a Varian Unity/Inova 300 MHz (^1H , 300 MHz; ^{31}P , 121 MHz) spectrometer or a 500 MHz (^1H , 500 MHz; ^{31}P , 202 MHz; ^{13}C , 126 MHz) spectrometer. The ^1H chemical shifts were referenced to the solvent peak or TMS (0.00 ppm). The ^{13}C chemical shifts were referenced to the solvent peak, and the ^{31}P chemical shifts were referenced externally to H_3PO_4 (0.00 ppm). Elemental analyses were conducted by Complete Analysis Laboratories, Inc. pH measurements were taken using an Accumet AB15 Basic pH meter. All hydration reaction samples were prepared in a glovebox under an atmosphere of N_2 in Wilmad 9 in. precision NMR tubes or in 1 dram screwcap vials fitted with septum caps. Reactions carried out in the Wilmad 9 in. NMR tubes were flame-sealed. Reaction tubes and vials were heated in an oil bath. Cyanohydrin hydration reactions were performed using a variety of reaction conditions. Representative procedures that gave the best results are given below.

Preparation of $[\text{Ru}(\eta^6\text{-}p\text{-cymene})\text{Cl}_2(\text{dmpmO})]$ (1-Me). $[\text{Ru}(\eta^6\text{-}p\text{-cymene})\text{Cl}_2]_2$ (0.083 g, 0.14 mmol) and dmpmO (0.11 g, 0.28 mmol) were dissolved in 10 mL of CH_2Cl_2 , and then the solution was stirred at room temperature for 4 h. The CH_2Cl_2 was removed under vacuum, and then hexanes was added to the orange solid, which was filtered over Celite. The solid was eluted off the Celite with CH_2Cl_2 . The product was precipitated from solution by addition of an excess of light petroleum ether and then filtered to obtain an orange powder (0.21 g, 73% yield). ^1H NMR (500 MHz, CDCl_3): δ 5.48 (q, $J = 6.2$ Hz, 4H), 2.84 (heptet, $J = 7.0$ Hz, 1H), 2.53 (dd, $J = 11.3$, 10.4 Hz, 2H), 2.07 (d, $J = 3.8$ Hz, 6H), 2.05 (s, 3H), 1.55 (dd, $J = 12.8$, 5.8 Hz, 6H), 1.23 (d, $J = 6.9$ Hz, 6H). ^{13}C NMR (151 MHz, CDCl_3): δ 107.43, 94.91, 89.55 (d, $J = 4.8$ Hz), 85.00 (d, $J = 6.1$ Hz), 30.74, 26.10 (dd, $J = 57.3$, 25.7 Hz), 22.11, 20.28 (d, $J = 69.8$ Hz), 18.36, 17.13 (d, $J = 31.7$ Hz). $^{31}\text{P}\{^1\text{H}\}$ NMR (202 MHz, CDCl_3): δ 37.93 (d, $J = 21.9$ Hz), 10.35 (d, $J = 20.6$ Hz) ppm. Anal. Found: C, 39.25; H, 6.06; P, 13.36. Calcd for $\text{C}_{13}\text{H}_{28}\text{Cl}_2\text{OP}_2\text{Ru}$: C, 39.51; H, 6.16; P, 13.52.

Preparation of $[\text{Ru}(\eta^6\text{-}p\text{-cymene})\text{Cl}_2(\text{dmpeO})]$ (2-Me). $[\text{Ru}(\eta^6\text{-}p\text{-cymene})\text{Cl}_2]_2$ (0.06 g, 0.098 mmol) and dmpeO (0.034 g, 0.2 mmol) were dissolved in 10 mL of CH_2Cl_2 , and then the solution was stirred at room temperature for 4 h. The CH_2Cl_2 was removed under vacuum, and then hexanes was added to the orange solid, which was filtered over Celite. The solid was eluted off the Celite with CH_2Cl_2 . The solid was precipitated from solution by addition of an excess of light petroleum ether and then filtered to obtain an orange powder (0.04 g, 47% yield). ^1H NMR (500 MHz, CDCl_3): δ 5.50 (q, $J = 5.9$ Hz, 4H), 2.83 (heptet, $J = 7.1$ Hz, 1H), 2.29 (m, 2H), 2.10 (s, 3H), 2.00 (m, 2H), 1.60 (d, $J = 10.5$ Hz, 6H), 1.52 (d, $J = 12.5$ Hz, 6H), 1.24 (d, $J = 6.9$ Hz, 6H). ^{13}C NMR (151 MHz, CDCl_3): δ 107.46, 94.71, 89.45 (d, $J = 4.5$ Hz), 85.12 (d, $J = 5.7$ Hz), 30.80, 25.95 (d, $J = 66.3$ Hz), 23.25 (dd, $J = 27.7$, 4.6 Hz), 22.20, 18.33, 16.36 (d, $J = 68.5$ Hz), 13.99 (d, J

= 32.3 Hz). $^{31}\text{P}\{^1\text{H}\}$ NMR (202 MHz, CDCl_3): δ 42.37 (d, J = 37.1 Hz), 11.98 (d, J = 39.7 Hz) ppm. Anal. Found: C, 40.60; H, 6.51; P, 12.97. Calcd for $\text{C}_{16}\text{H}_{30}\text{Cl}_2\text{OP}_2\text{Ru}$: C, 40.69; H, 6.40; P, 13.12.

Preparation of $[\text{Ru}(\eta^6\text{-}p\text{-cymene})\text{Cl}_2(\text{PMe}_2\text{OH})]$ (3-Me). $[\text{Ru}(\eta^6\text{-}p\text{-cymene})\text{Cl}_2]$ (0.40 g, 0.65 mmol) and dimethylphosphine oxide (0.26 g, 3.4 mmol) were dissolved in 10 mL of CH_2Cl_2 , and then the solution was stirred at room temperature for 12 h. The CH_2Cl_2 was removed under vacuum, and then hexanes was added to the orange solid, which was filtered over Celite. The solid was eluted off the Celite with CH_2Cl_2 . The solid was precipitated from solution by addition of an excess of light petroleum ether and then filtered to obtain an orange powder (0.42 g, 85% yield). ^1H NMR (500 MHz, CDCl_3): δ 5.50 (d, J = 5.7 Hz, 2H), 5.45 (d, J = 5.4 Hz, 2H), 2.91–2.72 (m, 1H), 2.10 (s, 3H), 1.93 (d, J = 9.5 Hz, 6H), 1.63 (dd, J = 13.8, 3.5 Hz, 1H), 1.23 (d, J = 6.9 Hz, 6H). ^{13}C NMR (151 MHz, CDCl_3): δ 107.12, 95.87, 89.41 (d, J = 5.0 Hz), 86.44 (d, J = 5.7 Hz), 30.79, 22.17 (d, J = 36.5 Hz), 22.14, 18.61. $^{31}\text{P}\{^1\text{H}\}$ NMR (202 MHz, CDCl_3): δ 115.33 ppm. Anal. Found: C, 37.45; H, 5.59; P, 7.93. Calcd for $\text{C}_{12}\text{H}_{21}\text{Cl}_2\text{OPRu}$: C, 37.51; H, 5.51; P, 8.06.

Preparation of $[\text{Ru}(\eta^6\text{-}p\text{-cymene})\text{Cl}_2(\text{P}(\text{OH})(\text{OEt})_2)]$ (3-OEt). $[\text{Ru}(\eta^6\text{-}p\text{-cymene})\text{Cl}_2]$ (0.23 g, 0.38 mmol) and diethylphosphine oxide (0.13 g, 0.97 mmol) were dissolved in 10 mL of CH_2Cl_2 , and then the solution was stirred at room temperature for 12 h. The CH_2Cl_2 was removed under vacuum and then hexanes were added to the orangeish solid, which was filtered over Celite. The product was eluted off the Celite with CH_2Cl_2 , precipitated from solution by addition of an excess of light petroleum ether, and then filtered to obtain an orange powder (0.26 g, 78% yield). ^1H NMR (500 MHz, CDCl_3): δ = 5.57 (d, J = 6.0 Hz, 2H), 5.44 (d, J = 6.1 Hz, 2H), 4.22 (p, J = 7.2 Hz, 4H), 2.97–2.72 (m, 1H), 2.17 (s, 3H), 1.34 (t, J = 7.1 Hz, 4H), 1.25 (d, J = 6.9 Hz, 4H). ^{13}C NMR (151 MHz, CDCl_3): δ 107.77, 101.28, 88.89, (d, J = 6.3 Hz), 88.21 (d, J = 5.6 Hz), 63.26 (d, J = 8.2 Hz), 30.84, 22.19, 18.75, 16.51 (d, J = 6.0 Hz). $^{31}\text{P}\{^1\text{H}\}$ NMR (202 MHz, CDCl_3): δ 111.79 ppm. Anal. Found: C, 37.93; H, 5.76; P, 6.79. Calcd for $\text{C}_{14}\text{H}_{25}\text{Cl}_2\text{O}_3\text{PRu}$: C, 37.85; H, 5.67; P, 6.97.

General Procedure for the Hydration of Acetonitrile. $[\text{Ru}(\eta^6\text{-}p\text{-cymene})\text{Cl}_2(\text{PR}_2\text{R}')] (0.02 \text{ mmol})$ was added to 2.8 mL of degassed D_2O in a 1 dram screwcap vial fitted with a septum cap. Dissolution of 3-Me or 3-OEt in water produces an acidic solution with pH 3.5, while solutions of 1 and 2 had a measured pH of 7.0. To this was added 0.45 mmol of acetonitrile to form a 150 mM nitrile solution. This solution was heated to 100 °C with stirring. Aliquots (0.1 mL) were removed periodically using a gastight syringe and then combined in an NMR tube with 0.6 mL of D_2O and 0.1 mL of a 3.8 mM NMe_4PF_6 in D_2O internal standard solution. The progress of the reaction was monitored by ^1H NMR spectroscopy by observing the disappearance of the acetonitrile resonance at 2.01 ppm (s, CH_3CN) and the appearance of acetamide at 1.93 ppm (s, $\text{CH}_3\text{C}(\text{O})\text{ND}_2$).

Hydration of Propionitrile. In a 1 dram screwcap vial fitted with a septum cap, propionitrile (22 μL , 0.31 mmol) was combined with $[\text{Ru}(\eta^6\text{-}p\text{-cymene})\text{Cl}_2(\text{PMe}_2\text{OH})]$ (1.9 mg, 0.005 mmol) and 2.03 mL of D_2O , forming a solution with pH 3.5. The solution was heated to 100 °C, and 0.1 mL aliquots were removed periodically and combined with 0.5 mL of d_6 -DMSO and 10 μL of 255 mM NMe_4PF_6 in d_6 -DMSO internal standard solution. The progress of the reaction was monitored by ^1H NMR spectroscopy by observing the disappearance of the propionitrile resonances at 2.54 (q, J = 7.6 Hz, 2H, $\text{CH}_3\text{CH}_2\text{CN}$) and 1.26 ppm (t, J = 7.6 Hz, 3H, $\text{CH}_3\text{CH}_2\text{CN}$) and the appearance of the propionamide resonances at 2.19 (q, J = 7.6 Hz, 2H, $\text{CH}_3\text{CH}_2\text{C}(\text{O})\text{ND}_2$) and 1.10 ppm (t, J = 7.6 Hz, 3H, $\text{CH}_3\text{CH}_2\text{C}(\text{O})\text{ND}_2$). Specific details for the hydration of other nitriles are described in the Supporting Information.

Hydration of Acetone Cyanohydrin. In a 1 dram screwcap vial fitted with a septum cap, $[\text{Ru}(\eta^6\text{-}p\text{-cymene})\text{Cl}_2(\text{PMe}_2\text{OH})]$ (10.7 μmol) was combined with 0.67 mL of H_2O and 0.77 mL of acetone, forming a solution with pH 3.5. Freshly distilled acetone cyanohydrin (20 μL , 0.22 mmol) was added to the solution, which was allowed to react at 25 °C, and 0.1 mL aliquots were removed periodically and combined with 0.5 mL of D_2O and 0.1 mL of 3.55 mM NMe_4PF_6 in D_2O . The progress of the reaction was monitored by ^1H NMR

spectroscopy by observing the disappearance of the methyl peak of acetone cyanohydrin at 1.57 ppm (s, 6H, $\text{HO}(\text{CH}_3)_2\text{CCN}$) and the appearance of the α -hydroxyisobutyramide resonance at 1.34 ppm (s, $\text{HO}(\text{CH}_3)_2\text{CC}(\text{O})\text{NH}_2$). Specific details for the hydration of other cyanohydrins are described in the Supporting Information.

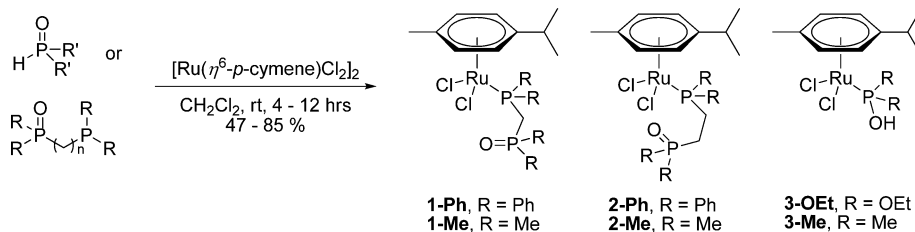
Titration with KCN. $[\text{Ru}(\eta^6\text{-}p\text{-cymene})\text{Cl}_2(\text{PMe}_2\text{OH})]$ (0.087 g, 0.23 mmol) was dissolved in 5.5 mL of degassed D_2O to form a 0.041 M stock solution, and KCN (0.11 g, 1.68 mmol) was dissolved in 1.0 mL of D_2O to form a 1.68 M stock solution. In a 1 dram screwcap vial fitted with a septum cap, aliquots of KCN dissolved in D_2O (0–110 μL ; 0–0.19 mmol, 0–50 mol %) were added to acetonitrile (19.5 μL , 0.37 mmol) and 0.45 mL of the $[\text{Ru}(\eta^6\text{-}p\text{-cymene})\text{Cl}_2(\text{PMe}_2\text{OH})]$ stock solution (0.019 mmol, 5 mol %). Each solution was heated to 100 °C with stirring. Aliquots (0.1 mL) were removed periodically using a gastight syringe and were combined in an NMR tube with 0.6 mL of D_2O and 0.1 mL of a 3.8 mM NMe_4PF_6 in D_2O internal standard solution. The progress of the reaction was monitored by ^1H NMR spectroscopy by observing the disappearance of the acetonitrile resonance at 2.01 ppm (s, CH_3CN) and the appearance of acetamide at 1.93 ppm (s, $\text{CH}_3\text{C}(\text{O})\text{ND}_2$).

Control Experiments for Ester Hydrolysis. $[\text{Ru}(\eta^6\text{-}p\text{-cymene})\text{Cl}_2(\text{PMe}_2\text{OH})]$ (0.014 g, 0.04 mmol) was dissolved in 1.5 mL of degassed D_2O to form a 0.025 M stock solution, and 3-(*N*-morpholino)propanesulfonic acid (MOPS, 0.20 g, 0.97 mmol) was dissolved in 3 mL of degassed D_2O to form a 0.32 M stock solution. The following solutions were made up in a 1 dram screwcap vial fitted with a septum cap: (1) 610 μL of $[\text{Ru}(\eta^6\text{-}p\text{-cymene})\text{Cl}_2(\text{PMe}_2\text{OH})]$ stock solution (0.015 mmol, 5 mol %) was combined with ethyl acetate (30 μL , 0.31 mmol) and 1.39 mL of D_2O to form a pH 3.5 solution; (2) 610 μL of $[\text{Ru}(\eta^6\text{-}p\text{-cymene})\text{Cl}_2(\text{PMe}_2\text{OH})]$ stock solution (0.015 mmol, 5 mol %) was combined with ethyl acetate (30 μL , 0.31 mmol), 200 μL of MOPS stock solution (0.065 mmol), and 1.20 mL of D_2O to form a pH 7.0 solution; (3) 1 M HCl was added dropwise to 3 mL of D_2O until pH 3.5 was measured and 2005 μL of this solution was combined with ethyl acetate (30 μL , 0.31 mmol) to form a pH 3.5 solution; (4) 200 μL of MOPS stock solution (0.065 mmol) was combined with ethyl acetate (30 μL , 0.31 mmol), and 1.80 mL of D_2O to form a pH 7.0 solution. Each solution was heated to 100 °C with stirring. Aliquots (0.1 mL) were removed periodically using a gastight syringe and were combined in an NMR tube with 0.6 mL of D_2O . The progress of the reaction was monitored by ^1H NMR spectroscopy by observing the disappearance of the ethyl acetate resonance at 1.17 ppm and the appearance of the ethanol resonance at 1.06 ppm. ^1H NMR (400 MHz, D_2O): ethyl acetate δ 4.03 ppm (q, 2H), 1.99 ppm (s, 3H), 1.17 ppm (t, 3H); ethanol δ 3.44 ppm (q, 2H), 1.06 ppm (t, 3H); acetic acid δ 1.91 ppm (s, 3H).

Computational Methods. Density functional theory (DFT) calculations were performed on the $[\text{Ru}(\eta^6\text{-}p\text{-cymene})\text{Cl}(\text{MeCN})\text{-(PMe}_2\text{OH)}\cdots\text{H-OH}]^+$ complex. Geometry optimizations were first performed on the complex without the water molecule. A water molecule was then added to promote hydrogen bonding to the PMe_2OH ligand, and the entire complex was optimized. Hydrogen bond distances were obtained from the optimized structures. Frequency calculations were performed on the optimized structures to confirm they were at a true minimum, and all yielded zero imaginary frequencies.

Modeling of the $[\text{Ru}(\eta^6\text{-}p\text{-cymene})\text{Cl}(\text{MeCN})\text{-(PMe}_2\text{OH)}\cdots\text{H-OH}]^+$ complex was done using the program Ecce v6.1.²⁰ Calculations were performed using NWChem version 6.0.²¹ For all atoms except ruthenium, the 6-311G** basis set²² was used for the geometry optimizations and frequency calculations. For ruthenium, the basis set and effective core potential developed by Andrae et al.,²³ augmented with one diffuse *f* function (ζ = 1.666) determined by Martin and Sundermann²⁴ and resulting in a (8s7p6d1f)/[6s5p3d1f] contraction, was used for both the optimizations and frequency calculations. All calculations employed the B3LYP functional.^{25–27}

X-ray Crystallography: General Methods. Structure determinations were performed on an Oxford Diffraction Gemini-R diffractometer, using Mo $K\alpha$ radiation (0.71073 Å). Single crystals were mounted on Hampton Research Cryoloops using Paratone-N oil.

Scheme 1. Synthesis of the $[\text{Ru}(\eta^6\text{-}p\text{-cymene})\text{Cl}_2(\text{PR}_2\text{R}')] \text{ Complexes}$ 

Unit cell determination, data collection and reduction, and analytical absorption correction were performed using the CrysAlisPro software package.²⁸ Direct methods structure solution was accomplished using SIR92²⁹ (**1-Me**) or Superflip³⁰ (**3-Me**), and full-matrix least-squares refinement was carried out using CRYSTALS.³¹

All non-hydrogen atoms were refined anisotropically. Hydrogen atoms were placed in calculated positions. Hydrogen positions were initially refined using distance and angle restraints and were fixed in place for the final refinement cycles.³² Crystallographic data for **1-Me** and **3-Me** and the details of data collection and refinement of the crystal structure are given in the Supporting Information.

Diffraction-quality crystals were obtained by slow diffusion of pentane into solutions of **1-Me** and **3-Me** in CH_2Cl_2 .

RESULTS AND DISCUSSION

Synthesis of the $[\text{Ru}(\eta^6\text{-}p\text{-cymene})\text{Cl}_2(\text{PR}_2\text{R}')] \text{ Complexes}$.

To explore the effect of the hydrogen bond accepting group position on the rate of nitrile hydration, the series of $[\text{Ru}(\eta^6\text{-arene})\text{Cl}_2(\text{PR}_2\text{R}')] \text{ catalysts}$ **1-Me**, **1-Ph**, **2-Me**, **2-Ph**, **3-Me**, and **3-OEt** was investigated (Scheme 1). The complexes $[\text{Ru}(\eta^6\text{-}p\text{-cymene})\text{Cl}_2(\text{dppmO})]$ (**1-Ph**) and $[\text{Ru}(\eta^6\text{-}p\text{-cymene})\text{Cl}_2(\text{dppeO})]$ (**2-Ph**) are known, having been previously investigated for their use as potential anticancer agents.³³ $[\text{Ru}(\eta^6\text{-arene})\text{Cl}_2\text{PR}_3]$ -type complexes with bulky phosphine ligands are slower nitrile hydration catalysts than catalysts with smaller phosphine ligands,⁸ and for that reason, the new, less bulky complexes **1-Me**, **2-Me**, **3-Me**, and **3-OEt** were also prepared. The respective reactions of dmpmO , dmppeO , $\text{Me}_2\text{P}(\text{O})\text{H}$, and $(\text{EtO})_2\text{P}(\text{O})\text{H}$ with $[\text{Ru}(\eta^6\text{-}p\text{-cymene})\text{Cl}_2]$ in CH_2Cl_2 at room temperature cleanly produced the monomeric complexes $[\text{Ru}(\eta^6\text{-}p\text{-cymene})\text{Cl}_2(\text{dmpmO})]$ (**1-Me**), $[\text{Ru}(\eta^6\text{-}p\text{-cymene})\text{Cl}_2(\text{dmppeO})]$ (**2-Me**), $[\text{Ru}(\eta^6\text{-}p\text{-cymene})\text{Cl}_2(\text{PMe}_2\text{OH})]$ (**3-Me**), and $[\text{Ru}(\eta^6\text{-}p\text{-cymene})\text{Cl}_2(\text{P}(\text{OEt})_2\text{OH})]$ (**3-OEt**) (Scheme 1). The complexes **1-Me**, **1-Ph**, **2-Me**, and **2-Ph** showed two doublet resonances in the ^{31}P NMR spectrum, where the signal corresponding to the phosphine is shifted upfield ($\Delta = 50\text{--}60$ ppm) relative to the free phosphine. The signal corresponding to the phosphine oxide is shifted downfield by 2–4 ppm, consistent with η^1 coordination of the bisphosphine monoxide ligand.³⁴ Complexes **3-OEt** and **3-Me** both showed a singlet ^{31}P NMR signal around 110 ppm, corresponding to P coordination of the phosphinite ligands.

The structures of compounds **1-Me** and **3-Me** were determined by X-ray diffraction methods. Figure 2 shows the structure of **1-Me**, and Figure 3 shows that of **3-Me**. Each complex adopts the expected three-legged “piano-stool” geometry. The Ru–P (2.3387(8) Å) and P–O (1.487(2) Å) bond lengths of **1-Me** are similar to those of **1-Ph** (2.355(7) Å and 1.49(1) Å)³⁵ and the related pendant oxide complex $[\text{Ru}(\eta^6\text{-}p\text{-cymene})\text{Cl}_2(\eta^1\text{-PPh}_2\text{CH}(\text{CH}_3)\text{P}(\text{O})\text{Ph}_2)]$ (2.374(1) and 1.484(3) Å).¹⁴ **3-Me** has a slightly shorter Ru–P bond

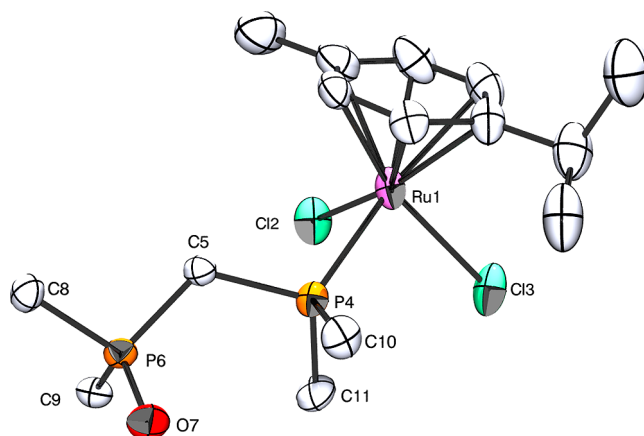


Figure 2. X-ray crystal structure of **1-Me**, showing 50% probability ellipsoids. Hydrogen atoms have been omitted for clarity. Selected metric data (bond lengths in Å and angles in deg): Ru(1)–Cl(2), 2.4219(8); Ru(1)–Cl(3), 2.3991(9); Ru(1)–P(4), 2.3387(8); Cl(2)–Ru(1)–Cl(3), 89.98(3); Cl(2)–Ru(1)–P(4), 82.56(3); Cl(3)–Ru(1)–P(4), 86.45(3); Ru(1)–C_{avg}, 2.211(4); Ru(1)–centroid, 1.705; P(4)–C(5), 1.828(3); P(6)–C(5), 1.817(3); P(4)–C(5)–P(6), 119.26(16); P(6)–O(7), 1.487(2).

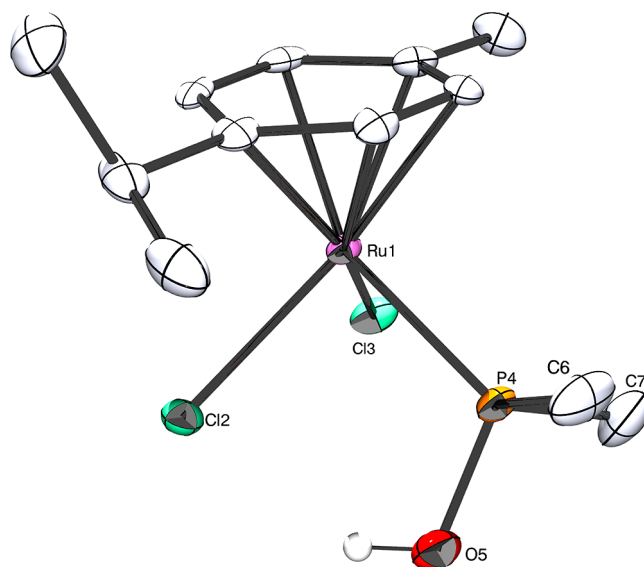


Figure 3. X-ray crystal structure of **3-Me**, showing 50% probability ellipsoids (selected molecule from the asymmetric cell). Hydrogen atoms have been omitted for clarity. Selected metric data (bond lengths in Å and angles in deg, averaged over asymmetric cell): Ru(1)–Cl(2), 2.4231(9); Ru(1)–Cl(3), 2.4160(5); Ru(1)–P(4), 2.3078(1); Cl(2)–Ru(1)–Cl(3), 87.00(8); Cl(2)–Ru(1)–P(4), 86.16(3); Cl(3)–Ru(1)–P(4), 86.51(3); Ru(1)–C_{avg}, 2.217(1); Ru(1)–centroid, 1.707; P(4)–O(5), 1.613(3).

Table 1. Hydration of Acetonitrile to Acetamide Catalyzed by $[\text{Ru}(\eta^6\text{-}p\text{-cymene})\text{Cl}_2(\text{PR}_2\text{R}')]$ and $[\text{Ru}(\eta^6\text{-}p\text{-cymene})\text{Cl}_2(\text{PR}_3)]$ Complexes in Water^a

entry	catalyst PR_3	TOF ^b	hydration (%)	reacn time (h)	$\text{Ni}(\text{CO})_3\text{PR}_3 \nu(\text{CO})$ (cm^{-1}) ^c	PR_3 cone angle (deg) ^{c,g}
1	dmpmO (1-Me)	0.054	92	331	~2063	~123
2	dmpeO (2-Me)	0.051	88	331	~2063	~123
3	dppmO (1-Ph)	0.033	56	331	~2067	~140
4	dppeO (2-Ph)	0.030	50	331	~2067	~140
5 ^d	PMe_2OH (3-Me)	31.95	98	0.9	2072 ^e (2006 for deprotonated form)	~118
6 ^d	$\text{P}(\text{OEt})_2\text{OH}$ (3-OEt)	0.96	5	1	2087 ^{e,f} (2028 for deprotonated form)	~109
7	$\text{P}(\text{OEt})_3$	0.01	18	26	2076.3	109
8 ^d	$\text{P}(\text{NMe}_2)_3$	25.3	97	1.1	2062	157

^aReactions were performed under an N_2 atmosphere at 100 °C and pH 7 using acetonitrile (0.15 M in water), with 5% catalyst loading. ^bTurnover frequencies ((mol of amide)/(mol of catalyst time)) were determined by taking the initial rate ((M amide)/time) divided by catalyst concentration (M). ^cElectronic and steric parameters for the various $\text{PR}_2\text{R}'$ ligands are taken from ref 38. ^dReactions were performed at pH 3.5. The pH of entry 8 was adjusted with HCl. Dissolution of 3-Me or 3-OEt in water produces an acidic solution with pH 3.5. ^eReference 39. ^fElectronic parameters are for the similar ligand $\text{P}(\text{OCH}_2\text{CH}_2\text{O})\text{OH}$. ^gThe cone angle and Tolman electronic parameter for the $\text{PR}_2\text{R}'$ ligands in 1-Ph and 2-Ph are assumed to be similar to those for PETPh_2 , and the cone angle and Tolman electronic parameter for the $\text{PR}_2\text{R}'$ ligands in 1-Me and 2-Me are assumed to be similar to those for PMe_2Et . The cone angles for the $\text{PR}_2\text{R}'$ ligands in 3-Me and 3-OEt are similar to those for PMe_3 and $\text{P}(\text{OEt})_3$.

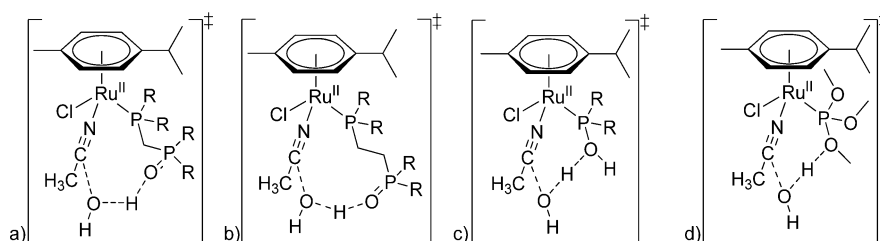


Figure 4. Transition state structures for the hydration of acetonitrile with (a) $[\text{Ru}(\eta^6\text{-}p\text{-cymene})\text{Cl}_2(\text{PR}_2(\text{CH}_2\text{P}(\text{O})\text{R}_2))]$ (1-Me and 1-Ph), (b) $[\text{Ru}(\eta^6\text{-}p\text{-cymene})\text{Cl}_2(\text{R}_2\text{P}(\text{CH}_2\text{CH}_2\text{P}(\text{O})\text{R}_2))]$ (2-Me and 2-Ph), (c) $[\text{Ru}(\eta^6\text{-}p\text{-cymene})\text{Cl}_2(\text{PR}_2(\text{OH}))]$ (3-Me and 3-OEt), and (d) $[\text{Ru}(\eta^6\text{-}p\text{-cymene})\text{Cl}_2(\text{P}(\text{OMe})_3)]$. The transition state ring sizes for each are 7, 9, 10, and 7 for a–d, respectively.

length (2.3078(1) Å) and a longer P–O bond length (1.613(3) Å), consistent with a P–O single bond.

Secondary Coordination Sphere H-Bonding Effects.

The effect on catalyst activity of the position of the H bond accepting group in the secondary coordination sphere was investigated by hydrating acetonitrile using 1-Me, 1-Ph, 2-Me, 2-Ph, 3-Me, and 3-OEt as catalysts. Of the complexes investigated, 3-Me was by far the best catalyst, with a turnover frequency (TOF) of 31.95 h^{-1} (Table 1).³⁶ 3-OEt had the second highest activity with a TOF of 0.96 h^{-1} . Complexes 2-Ph, 1-Ph, 2-Me, and 1-Me had much lower catalytic activity, with TOFs of 0.030, 0.033, 0.051, and 0.053 h^{-1} , respectively. Previous work with the $[\text{Ru}(\eta^6\text{-}p\text{-cymene})\text{Cl}_2\text{PET}_3]$ and $[\text{Ru}(\eta^6\text{-}p\text{-cymene})\text{Cl}_2\text{P}^i\text{Pr}_3]$ catalysts showed that nitrile hydration is faster with less bulky phosphines,⁸ and the general trend observed in Table 1 is consistent with this prior finding. Thus, catalysts 1-Ph and 2-Ph are the slowest because they have the bulkiest ligands, catalysts 1-Me and 2-Me have smaller $\text{PR}_2\text{R}'$ ligands than 1-Ph and 2-Ph and are therefore slightly faster, and 3-Me and 3-OEt have the smallest phosphines and are the fastest. (The exception to this ordering is that 3-Me is faster than 3-OEt, despite the fact that 3-Me is the sterically bulkier ligand. Reasons for this deviation are discussed below.) Previous work also showed that the rate decreased with increasing electron-donating ability of the ligands on the catalyst. The general trend in the rates for the catalysts in Table 1 also follow this general rule, but the changes in electron-donating ability (as indicated by the Tolman $\nu(\text{CO})$ parameter) are small, and it is suggested that the major influence on the rate is the steric bulkiness of the $\text{PR}_2\text{R}'$ ligand.³⁷

If the steric properties (and to a lesser extent the electronic properties) of the ligand solely determine the efficiency of the catalysts, then 3-OEt should be faster than 3-Me (because $\text{P}(\text{OEt})_2\text{OH}$ is less bulky than PMe_2OH and because PMe_2OH is a better donor than $\text{P}(\text{OEt})_2\text{OH}$; see Table 1). However, 3-Me is a far better catalyst, and the implication is that other factors are also important in determining the rate. It is suggested that the superior catalytic ability of 3-Me in comparison to 3-OEt is due to the H bonding that occurs in the secondary coordination sphere between the $\text{PR}_2\text{R}'$ ligand and the entering water nucleophile (Figure 4). Although $\text{P}(\text{OEt})_2\text{OH}$ could potentially H bond to water, the electron-withdrawing inductive effect of the OEt groups will decrease the electron density on the O(H) atom in $\text{P}(\text{OEt})_2\text{OH}$, making this O atom a poorer H bond acceptor than the corresponding O atom in the PMe_2OH ligand.

The very low TOFs with catalysts 1-Me, 1-Ph, 2-Me, and 2-Ph likely indicate that H bonding to the nucleophilic water is not occurring with these catalysts. This result is not surprising. The activation of water by H bonding in the secondary coordination sphere results in the formation of a cyclic transition state in the rate-limiting step (Figures 1 and 4). It is well-established that ring-forming reactions became more entropically favorable as the ring size increases from 3- to 6-membered rings, then less favorable as the ring size increases from 7- to 10-membered rings, with 5-, 6-, and 7-membered rings being the most favorable.^{40,41} It is also known that the strength of H bonding interactions is sensitive to entropy.⁴² Consequently, in H bonding situations involving the formation of a cyclic transition state, the rate of the reaction will decrease as the ring-forming reaction becomes less entropically

favorable. **3-Me** and the previously investigated complex $[\text{Ru}(\eta^6\text{-}p\text{-cymene})\text{Cl}_2\text{P}(\text{NMe}_2)_3]$ (which has a comparable rate; Table 1) would form 7-membered transition states, which are more favorable than the 9- and 10-membered rings that form in the transition state with catalysts **1-Me**, **1-Ph**, **2-Me**, and **2-Ph**.

It might be argued that the decreased activity of **1-Me**, **1-Ph**, **2-Me**, and **2-Ph** may simply be due to the ability of the phosphine oxide group to coordinate to the ruthenium, making the $\text{R}_2\text{P}(\text{CH}_2)_n\text{P}(\text{O})\text{R}_2$ ($\text{R} = \text{Ph}, \text{Me}$ and $n = 1, 2$) ligands bidentate (Figure 5).¹⁴ This type of η^2 coordination through

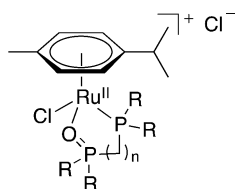


Figure 5. Structure of the bidentate complex $[\text{Ru}(\eta^6\text{-}p\text{-cymene})\text{Cl}(\eta^2\text{-R}_2\text{P}(\text{CH}_2)_n\text{P}(\text{O})\text{R}_2)]\text{Cl}$, where $\text{R} = \text{Ph}, \text{Me}$ and $n = 1, 2$.

the phosphine oxide was previously shown for the related complex $[\text{Ru}(\eta^6\text{-}p\text{-cymene})\text{Cl}_2(\eta^1\text{-PPh}_2\text{CH}(\text{R}')\text{P}(\text{O})\text{Ph}_2)]$ ($\text{R}' \neq \text{H}$) in polar solutions, where equilibrium mixtures of the bidentate and monodentate complexes were observed. It is noted that complexes with bulkier R' groups in the methylene position showed greater concentrations of the bidentate complex at equilibrium.¹⁴ Crucially, the bidentate complex was not observed for **1-Ph**,¹⁴ and therefore the bidentate complex is also not expected to form for **1-Me** and, by extrapolation, for **2-Me** because both are less sterically bulky than **1-Ph** and **2-Ph**.

To summarize this section, the general trend in catalyst rates is primarily determined by the steric properties of the $\text{PR}_2\text{R}'$ ligand in the $\text{Ru}(\eta^6\text{-}p\text{-cymene})\text{Cl}_2(\text{PR}_2\text{R}')$ -type complexes. However, ligands with an OH group bonded to the P atom (as in **3-Me** and **3-OEt**) are faster catalysts, which is probably attributable to their ability to activate the water nucleophile by forming a relatively stable, cyclic, H bonded transition state. The location of the H bond acceptor atom is crucial. When the formation of an H bond results in a large ring, the rate is not enhanced, likely due to the entropic unfavorability of forming the large ring.

DFT Analysis of Nitrile Hydration. The hydrogen bond accepting ability of $[\text{Ru}(\eta^6\text{-}p\text{-cymene})\text{Cl}(\text{MeCN})(\text{PMe}_2\text{OH})]^+$ was investigated by DFT analysis at the 6-311G** level of theory. The $\text{H}\cdots\text{O}$ (ligand) and $\text{O}\cdots\text{C}$ (nitrile) bond lengths in the cyclic transition state (Figure 4c) were calculated and compared to prior results obtained for the complexes $[\text{Ru}(\eta^6\text{-}p\text{-cymene})\text{Cl}(\text{MeCN})(\text{P}(\text{NMe}_2)_3)]^+$ and $[\text{Ru}(\eta^6\text{-}p\text{-cymene})\text{Cl}(\text{MeCN})(\text{P}(\text{OMe})_3)]^+$ (Table 2).^{8,13} The calculations showed that the complex $[\text{Ru}(\eta^6\text{-}p\text{-cymene})\text{Cl}(\text{MeCN})(\text{P}(\text{OMe})_3)]^+$, which is the slowest nitrile hydration catalyst of the three, has the longest bond distances. The bond lengths in the catalysts $[\text{Ru}(\eta^6\text{-}p\text{-cymene})\text{Cl}(\text{MeCN})(\text{P}(\text{NMe}_2)_3)\cdots\text{H}-\text{OH}]^+$ and $[\text{Ru}(\eta^6\text{-}p\text{-cymene})\text{Cl}(\text{MeCN})(\text{PMe}_2\text{OH})\cdots\text{H}-\text{OH}]^+$ are shorter, implying greater hydrogen bonding and consistent with their faster activity.

Nitrile Hydration with 3-Me. Because **3-Me** was the fastest catalyst for CH_3CN hydration, its activity toward other nitriles was investigated (Figure 6). Propionitrile, isobutyronitrile, trimethylacetone nitrile, and benzonitrile were investigated to

Table 2. Calculated Binding Energies and H-Bond Lengths of the $[\text{P}(\text{R})_3\cdots\text{H}-\text{OH}]$ Free Ligand^a and the Corresponding $[\text{Ru}(\eta^6\text{-}p\text{-cymene})\text{Cl}(\text{MeCN})(\text{PR}_3)\cdots\text{H}-\text{OH}]^+$ Complexes using 6-311G**(B3LYP)

complex	H bond length (Å)	$\text{H}_2\text{O}\cdots\text{MeCN}$ dist (Å) ^b
$[\text{P}(\text{NMe}_2)_3\cdots\text{H}-\text{OH}]^c$	2.016	
$[\text{P}(\text{OMe})_3\cdots\text{H}-\text{OH}]^c$	2.012	
$[\text{PMe}_2\text{OH}\cdots\text{H}-\text{OH}]$	1.957	
$[\text{Ru}(\eta^6\text{-}p\text{-cymene})\text{Cl}(\text{MeCN})\text{P}(\text{NMe}_2)_3\cdots\text{H}-\text{OH}]^+{}^c$	1.974	2.923
$[\text{Ru}(\eta^6\text{-}p\text{-cymene})\text{Cl}(\text{MeCN})\text{P}(\text{OMe})_3\cdots\text{H}-\text{OH}]^+{}^c$	2.038	3.005
$[\text{Ru}(\eta^6\text{-}p\text{-cymene})\text{Cl}(\text{MeCN})(\text{PMe}_2\text{OH})\cdots\text{H}-\text{OH}]^+$	2.014	2.942

^aThe water is hydrogen bonded to the heteroatom on the free phosphine ligand. ^bThis describes the calculated distance between the oxygen of the water that is hydrogen bonded to the coordinated phosphine ligand and the nitrile carbon of the coordinated acetonitrile. See the structures in Figure 4. ^cSee ref 8.

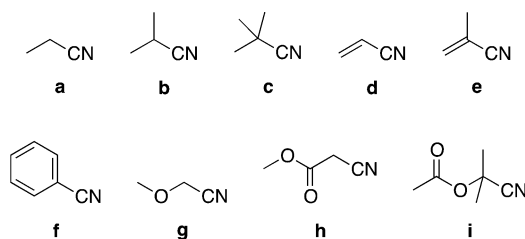


Figure 6. Nitriles hydrated with **3-Me**: (a) propionitrile; (b) isobutyronitrile; (c) trimethylacetone nitrile; (d) acrylonitrile; (e) methacrylonitrile; (f) benzonitrile; (g) methoxyacetone nitrile; (h) methyl cyanoacetate; (i) acetone cyanohydrin acetate.

probe the effect of nitrile bulk on catalyst activity. These nitriles were hydrated with TOFs of 14.0, 3.0, 6.1, and 20.7 h^{-1} , respectively (Table 3). The general trend is for decreased TOF with increasing steric bulk in the nitrile, but the cause of the reduced activity with **3-Me** toward isobutyronitrile is not known. In this case, the catalyst solution turned gray as hydration progressed, indicating that the catalyst mixture may not remain homogeneous.

The hydration reactions of acrylonitrile, methacrylonitrile, methylcyanoacetate, and acetone cyanohydrin acetate with **3-Me** were also investigated because ester and alkene functional groups are known to be susceptible to hydration or hydrolysis in the presence of some nitrile hydration catalysts.⁹ The $\text{C}\equiv\text{N}$ groups in acrylonitrile and methacrylonitrile were completely hydrated, and no alkene hydration or polymerization was observed. Some (~5%) ester hydrolysis was observed during the hydration of methyl cyanoacetate (Table 1, entry 9), as indicated by the formation of methanol in the NMR spectrum. However, the hydration of the resulting mixture of methyl cyanoacetate and its hydrolyzed cyanoacetic acid went to completion. The $\text{P}-\text{O}-\text{H}$ group has a $\text{p}K_a$ of 4.11 ± 0.08 , meaning that at pH 3.5 approximately one-third of the catalyst in solution is deprotonated. Because the hydration reactions with **3-Me** were carried out at pH 3.5, the ester hydrolysis may be catalyzed by the acid in solution, rather than by **3-Me**. To investigate this hypothesis, control hydrolysis reactions of ethyl acetate were carried out at pH 3.5 (100 °C) both with catalyst (5 mol % of **3-Me**) and without catalyst. In addition, control hydrolysis reactions of ethyl acetate were carried out at pH 7.0

Table 3. Selected Nitrile Hydration Results Using $[\text{Ru}(\eta^6\text{-}p\text{-cymene})\text{Cl}_2(\text{P}(\text{OH})\text{Me}_2)]^a$

entry	substrate	[substrate] (mM)	[catalyst] (mM)	pH	hydration (%) ^b	reacn time (h)
1	acetonitrile	150.8	7.6	3.5	98	1.0
2	propionitrile	150.3	7.5	3.5	93	2.2
3	isobutyronitrile	150.2	7.5	3.5	74	7.5
4	trimethylacetone nitrile	149.0	7.5	3.5	90	7.5
5	acrylonitrile	150.0	7.5	3.5	>99	2.0
6	methacrylonitrile	149.7	7.5	3.5	98	3.0
7	benzoxynitrile	150.2	7.5	3.5	>99	2.0
8	methoxyacetone nitrile	152.3	7.6	3.5	>99	1.0
9	methyl cyanoacetate	150	7.5	3.5	>99 (5% ester hydrolysis)	2.0
10	methyl cyanoacetate	150.2	7.5	7.0	>99 (25% ester hydrolysis)	1.7
11	ethyl acetate	150.7	7.5	3.5	46	1.8
12	ethyl acetate	150.7	7.5	7.0	26	1.8
13	ethyl acetate	150.7	0	3.5	46	1.8
14	ethyl acetate	150.7	0	7.0	0	1.8

^aReactions performed under an N₂ atmosphere in D₂O with 5% catalyst loading at 100 °C. ^bYields determined by ¹H NMR. No formation of carboxylic acid byproduct was observed in any hydration trial, and no deuteration of C–H protons was observed in any hydration trial.

Table 4. Selected Cyanohydrin Hydration Results^a Using $[\text{Ru}(\eta^6\text{-}p\text{-cymene})\text{Cl}_2(\text{P}(\text{NMe}_2)_3)]^b$ or $[\text{Ru}(\eta^6\text{-}p\text{-cymene})\text{Cl}_2(\text{PMe}_2\text{OH})]$

entry	cyanohydrin	catalyst PR ₃	[cosolvent] (M)	[catalyst] (mM)	calcd [HCN] at equilibrium (mM) ^c	hydration (%) ^d	reacn time (h)
1	glycolonitrile	PMe ₂ OH		7.5	0.01	>99	6.2
2 ^e	glycolonitrile	P(NMe ₂) ₃		7.6	0.07	>99	49
3	lactonitrile	PMe ₂ OH		7.5	2.01	94	17.5
4	lactonitrile	P(NMe ₂) ₃		7.6	2.01	>99	112
5	ACH	PMe ₂ OH	11.6	7.5	0.93	3.3	0.8
6	ACH	PMe ₂ OH	7.2	7.5	1.48	6.5	1.0
7	ACH	PMe ₂ OH	5.0	7.4	2.10	3.9	1.1
8 ^f	ACH	P(NMe ₂) ₃	10.6	7.5	1.01	14	149
9	acetone cyanohydrin acetate	PMe ₂ OH		7.5		60.6	2.0 (100 °C)
10 ^g	acetone cyanohydrin acetate	PMe ₂ OH		7.4		>99	3.7 (100 °C)

^aReactions performed under an N₂ atmosphere in D₂O at 25 °C with 0.15 M cyanohydrin, 5% catalyst loading, and pH 3.5. ACH hydrations conducted with acetone cosolvent. ^bSee ref 7. ^cConcentration of cyanide at equilibrium was calculated using published equilibrium constants.³ ^dYields determined by ¹H NMR. No formation of carboxylic acid byproduct was observed in any hydration trial, and no deuteration of C–H protons was observed in any hydration trial. ^eReaction done at pH 8.5. ^fReaction done at pH 3.0. ^gReaction done at pH 7.0.

(100 °C) both with catalyst (5 mol % of **3-Me**) and without catalyst. At pH 3.5, the catalyst had no effect on the extent of hydrolysis; 46% of ethyl acetate was hydrolyzed to acetic acid and ethanol in each trial (Table 3, entries 11 and 13; see the Supporting Information for details).⁴³ In comparison, the catalyst does have an effect at pH 7: no hydrolysis was observed in the absence of catalyst (Table 3, entry 14), but 26% hydrolysis occurred with the catalyst present (Table 3, entry 12). The ability of **3-Me** to function as a hydrolysis catalyst at pH 7 likely explains the more extensive ester hydrolysis observed at pH 7 than at pH 3.5 for the hydration of methyl cyanoacetate (Table 3, entries 9 and 10).

Hydration of Cyanohydrins. The hydration of the cyanohydrins glycolonitrile, lactonitrile, and acetone cyanohydrin was investigated with **3-Me**. Previous investigations with the $[\text{Ru}(\eta^6\text{-}p\text{-cymene})\text{Cl}_2(\text{P}(\text{NMe}_2)_3)]$ catalyst showed that the optimal conditions for cyanohydrin hydration are low temperatures (25 °C) and low pH (3–4). Acetone cyanohydrin hydration also requires the use of acetone cosolvent.^{4,7,8} The results of the cyanohydrin hydrations with **3-Me** at 25 °C, pH 3.5, 5% catalyst loading, and 150 mM nitrile are shown in Table 4.

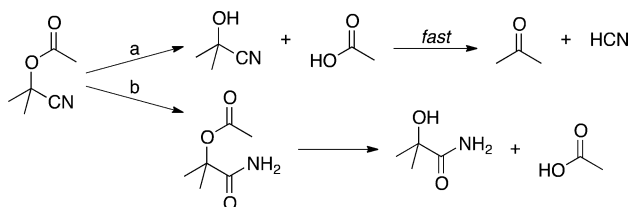
Under these conditions, glycolonitrile and lactonitrile hydration both went to completion within 6.2 and 17.5 h

with >99% and 94% yields, respectively (Table 4). These results correlate with the superior catalytic activity of **3-Me** in comparison to $[\text{Ru}(\eta^6\text{-}p\text{-cymene})\text{Cl}_2(\text{P}(\text{NMe}_2)_3)]$ at pH 3.5.

The hydration of acetone cyanohydrin, by comparison, was worse than expected. Under all conditions in which the hydration was attempted, no more than 4% conversion of acetone cyanohydrin to 2-hydroxyisobutyramide was observed (Table 4, entries 5–7). It is suggested that this low conversion is likely due to a higher sensitivity of **3-Me** to cyanide, as shown by cyanide poisoning studies (see below).

To limit the degradation of acetone cyanohydrin, the alcohol group on acetone cyanohydrin was protected by acetate. Hydration of acetone cyanohydrin acetate with **3-Me** at pH 3.5 and 100 °C gave a 60% conversion to a mixture of the desired α -hydroxyisobutyramide and α -acetoxyisobutyramide products (Table 4, entry 9). However, hydrolysis of the acetone cyanohydrin acetate also occurred to form acetone cyanohydrin (Scheme 2a), which degraded and subsequently caused the catalyst activity to cease due to cyanide poisoning. The previous control studies with ethyl acetate showed that the rate of ester hydrolysis was significantly decreased at higher pH; therefore, the hydration of acetone cyanohydrin acetate was also carried out at pH 7.0. Under these conditions, complete hydration of acetone cyanohydrin acetate occurred, with the amide products

Scheme 2. (a) Hydrolysis of Acetone Cyanohydrin Acetate, Reforming Acetone Cyanohydrin, Which Quickly Degrades To Form Cyanide, and (b) Hydration of Acetone Cyanohydrin Acetate to α -Acetoxyisobutyramide, Which May Be Hydrolyzed To Form α -Hydroxyisobutyramide



being a mixture of α -hydroxyisobutyramide and α -acetoxyisobutyramide (Table 4, entry 10; Scheme 2b).

Catalyst Inhibition Tests. Previous control experiments with the $\text{PtCl}(\text{PMe}_2\text{OH})(\text{PMe}_2\text{O})_2\text{H}$ catalyst showed that as the $[\text{KCN}]/[\text{PtCl}(\text{PMe}_2\text{OH})(\text{PMe}_2\text{O})_2\text{H}]$ ratio increased, the rate of acetonitrile hydration decreased because of cyanide poisoning.⁶ To determine if cyanide similarly inhibits the nitrile hydration activity of **3-Me**, aliquots of potassium cyanide were added to acetonitrile hydration solutions. Interestingly, the rate of hydration did not decrease linearly, as was observed previously with $[\text{PtCl}(\text{PMe}_2\text{OH})(\text{PMe}_2\text{O})_2\text{H}]$.⁶ Instead, as the number of equivalents of cyanide increased from 0 to 1, the rate of acetonitrile hydration increased. Only after 1 equiv of cyanide was added did the rate of hydration decrease, and all catalyst activity practically ceased with 5 equiv of cyanide (Figure 7).

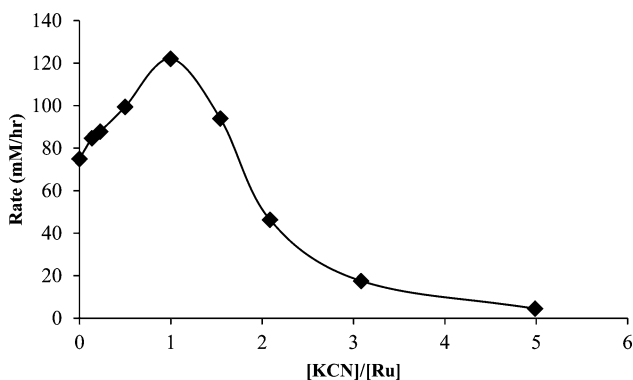
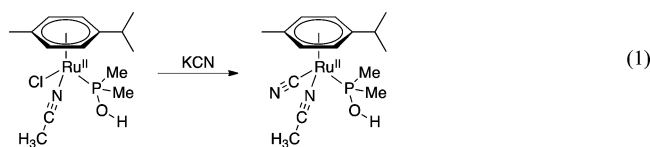


Figure 7. Plot of acetonitrile hydration rate versus $[\text{KCN}]/[\text{Ru}]$ showing the effect of added cyanide on the catalytic activity of $[\text{Ru}(\eta^6\text{-}p\text{-cymene})\text{Cl}_2(\text{PMe}_2\text{OH})]$.

To explain this behavior, it is proposed that the active catalyst during acetonitrile hydration in the absence of cyanide is $[\text{Ru}(\eta^6\text{-}p\text{-cymene})\text{Cl}(\text{NCMe})(\text{PMe}_2\text{OH})]$.⁴⁴ Addition of 1 equiv of cyanide yields the complex $[\text{Ru}(\eta^6\text{-}p\text{-cymene})(\text{CN})(\text{NCMe})(\text{PMe}_2\text{OH})]^+$ (eq 1), which is likely a faster catalyst



than its chloro or aquo precursor because the cyanide ligand is more electron withdrawing than chloride or water and can therefore better activate nitriles for hydration.

SUMMARY

With the catalysts **1-Me**, **1-Ph**, **2-Me**, **2-Ph**, **3-Me**, and **3-OEt**, the general trend in nitrile hydration rates is primarily determined by the steric properties of the $\text{PR}_2\text{R}'$ ligands. However, the proper placement of an H bond accepting group in the $\text{PR}_2\text{R}'$ ligand can effect the rate. The TOF is faster if the cyclic, H bonded transition state (Figures 1 and 4) is entropically favored. For example, the transition states formed with **3-Me** and **3-OEt** have 7 total atoms, and these catalysts are faster than reactions with **1-Me**, **1-Ph**, **2-Me**, and **2-Ph**, where 9- and 10-membered rings are formed. Although the catalysts **3-Me** and **3-OEt** both form transition states with 7 atoms, the faster rate for **3-Me** is attributed to the greater H bond accepting ability of the PMe_2OH ligand in comparison to the $\text{P}(\text{OEt})_2\text{OH}$ ligand.

Catalyst **3-Me** was able to hydrate a variety of nitriles, including several cyanohydrins. In fact, **3-Me** was a faster catalyst for the hydration of glycolonitrile and lactonitrile (both cyanohydrins) than $[\text{Ru}(\eta^6\text{-}p\text{-cymene})\text{Cl}_2\text{P}(\text{NMe}_2)_3]$, the best previously investigated homogeneous cyanohydrin hydration catalyst.^{7,8} Unfortunately, as was the case with the other previously studied homogeneous nitrile hydration catalysts, the catalysts investigated here are susceptible to cyanide poisoning. Thus, **3-Me** was not a good acetone cyanohydrin hydration catalyst for this reason. What is abundantly clear is that homogeneously catalyzed acetone cyanohydrin hydration will never be viable unless a way can be found to eliminate cyanide poisoning. One strategy to prevent catalyst poisoning is to protect the $-\text{OH}$ group of the cyanohydrin, and in fact this strategy does work: protecting acetone cyanohydrin with an acetate group quantitatively gave the hydration product at pH 7 and with >60% yield at pH 3.5. Of course, protecting the $-\text{OH}$ group may not be industrially viable. Another strategy to prevent catalyst poisoning is to use a catalyst with labile metal–cyanide bonds; our next paper will report the results of using this approach.

ASSOCIATED CONTENT

Supporting Information

Text, figures, and CIF files giving experimental details for the hydration of nitriles and cyanohydrins with **3-Me**, ^1H , ^{31}P , and ^{13}C NMR spectra of dmpeO , dmpmO , and catalysts **1-Me**, **2-Me**, **3-Me**, and **3-OEt**, crystallographic data for **1-Me** and **3-Me** and details of the data collection and refinement of the crystal structures, and time course data for the hydrolysis of ethyl acetate and the hydration and hydrolysis of acetone cyanohydrin acetate at pH 3.5 and 7.0. This material is available free of charge via the Internet at <http://pubs.acs.org>.

AUTHOR INFORMATION

Corresponding Author

*E-mail for D.R.T.: dtyler@uoregon.edu.

Present Address

[§]Department of Chemistry, Colgate University, Hamilton, NY 13346.

Notes

The authors declare no competing financial interest.

ACKNOWLEDGMENTS

We thank Anthony R. Chianese at Colgate University for his help in obtaining the X-ray crystal structures. We would also like to thank Rohm and Haas Chemical Co. and the NSF

(CHE-0719171) for the support of research carried out in the authors' laboratory. X-ray structure determination was supported by the NSF (CHE-1057792 and CHE-0819686). S.M.M.K. also acknowledges the U.S. Department of Education (P200A070436) and the NSF Graduate STEM Fellows in K-12 Education (GK-12) program (DGE-0742540) for additional support. "Extensible Computational Chemistry Environment (ECCE), A Problem Solving Environment for Computational Chemistry, Software Version 6.1" (2011), as developed and distributed by Pacific Northwest National Laboratory, P.O. Box 999, Richland, WA 99352, USA, and funded by the U.S. Department of Energy, was used to obtain some of these results.

REFERENCES

- (1) Nagai, K. *Appl. Catal., A* **2001**, *221*, 367–377.
- (2) Green, M. M.; Wittcoff, H. A. In *Organic Chemistry Principles and Industrial Practice*; Wiley-VCH: Weinheim, Germany, 2003; pp 137–156.
- (3) Schlesinger, G.; Miller, S. L. *J. Am. Chem. Soc.* **1973**, *95*, 3729–3735.
- (4) Stewart, T. D.; Fontana, B. J. *J. Am. Chem. Soc.* **1940**, *62*, 3281–3285.
- (5) Yates, W. F.; Heider, R. L. *J. Am. Chem. Soc.* **1952**, *74*, 4153–4155.
- (6) Ahmed, T. J.; Fox, B. R.; Knapp, S. M. M.; Yelle, R. B.; Juliette, J. J.; Tyler, D. R. *Inorg. Chem.* **2009**, *48*, 7828–7837.
- (7) Knapp, S. M. M.; Sherbow, T. J.; Juliette, J. J.; Tyler, D. R. *Organometallics* **2012**, *31*, 2941–2944.
- (8) Knapp, S. M. M.; Sherbow, T. J.; Yelle, R. B.; Zakharov, L. N.; Juliette, J. J.; Tyler, D. R. *Organometallics* **2013**, *32*, 824–834.
- (9) Ahmed, T. J.; Knapp, S. M. M.; Tyler, D. R. *Coord. Chem. Rev.* **2011**, *255*, 949–974.
- (10) Kukushkin, V. Y.; Pombeiro, A. J. L. *Inorg. Chim. Acta* **2005**, *358*, 1–21.
- (11) García-Álvarez, R.; Díez, J.; Crochet, P.; Cadierno, V. *Organometallics* **2010**, *29*, 3955–3965.
- (12) Lee, W.-C.; Sears, J. M.; Enow, R. A.; Eads, K.; Krogstad, D. A.; Frost, B. J. *Inorg. Chem.* **2013**, *52*, 1737–1746.
- (13) Steiner, T. *Angew. Chem., Int. Ed.* **2002**, *41*, 48–76.
- (14) Faller, J. W.; Patel, B. P.; Albrizzio, M. A.; Curtis, M. *Organometallics* **1999**, *18*, 3096–3104.
- (15) Boshala, A. M. A.; Simpson, S. J.; Autschbach, J.; Zheng, S. *Inorg. Chem.* **2008**, *47*, 9279–9292.
- (16) Hays, H. R. *J. Org. Chem.* **1968**, *33*, 3690–3694.
- (17) Clement, J.-L.; Finet, J.-P.; Frejaville, C.; Tordo, P. *Org. Biomol. Chem.* **2003**, *1*, 1591–1597.
- (18) Hiyama, T.; Oishi, H.; Suetsugu, Y.; Nishide, K.; Saimoto, H. *Bull. Chem. Soc. Jpn.* **1987**, *60*, 2139–2150.
- (19) Mäding, P.; Scheller, D. *Z. Anorg. Allg. Chem.* **1988**, *567*, 179–191.
- (20) Black, G.; Chase, J.; Chatterton, J.; Daily, J.; Elsethagen, T.; Feller, D.; Gracio, D.; Jones, D.; Keller, T.; Lansing, C.; Matsumoto, S.; Palmer, B.; Peterson, M.; Schuchardt, K.; Stephan, E.; Sun, L.; Swanson, K.; Taylor, H.; Thomas, G.; Vorpagel, E.; Windus, T.; Winters, C. *ECCE, A Problem Solving Environment for Computational Chemistry, Software Version 6.3*; Pacific Northwest National Laboratory: Richland, WA 99352-0999, USA, 2011.
- (21) Valiev, M.; Bylaska, E. J.; Govind, N.; Kowalski, K.; Straatsma, T. P.; Van Dam, H. J. J.; Wang, D.; Nieplocha, J.; Apra, E.; Windus, T. L.; de Jong, W. A. *Comput. Phys. Commun.* **2010**, *181*, 1477–1489.
- (22) Krishnan, R.; Binkley, J. S.; Seeger, R.; Pople, J. A. *J. Chem. Phys.* **1980**, *72*, 650–654.
- (23) Andrae, D.; Häußermann, U.; Dolg, M.; Stoll, H.; Preuß, H. *Theor. Chem. Acc.* **1990**, *77*, 123–141.
- (24) Martin, J. M. L.; Sundermann, A. *J. Chem. Phys.* **2001**, *114*, 3408–3420.
- (25) Becke, A. D. *Phys. Rev. A* **1988**, *38*, 3098–3100.
- (26) Becke, A. D. *J. Chem. Phys.* **1993**, *98*, 5648–5652.
- (27) Becke, A. D. *J. Chem. Phys.* **1993**, *98*, 1372–1377.
- (28) *CrysAlisPro Software system, Version 1.171.32 and Xcalibur CCD system*; Oxford Diffraction Ltd., 2007.
- (29) Altomare, A.; Casciarano, M.; Giacovazzo, C.; Guagliardi, A.; Burla, M. C.; Polidori, G.; Camalli, M. *J. Appl. Crystallogr.* **1994**, *27*, 435–436.
- (30) Palatinus, L.; Chapuis, G. *J. Appl. Crystallogr.* **2007**, *40*, 786–790.
- (31) Betteridge, P. W.; Carruthers, J. R.; Cooper, R. I.; Prout, K.; Watkin, D. J. *J. Appl. Crystallogr.* **2003**, *36*, 1487.
- (32) Cooper, R. I.; Thompson, A. L.; Watkin, D. J. *J. Appl. Crystallogr.* **2010**, *43*, 1100–1107.
- (33) Das, S.; Sinha, S.; Britto, R.; Somasundaram, K.; Samuelson, A. G. *J. Inorg. Biochem.* **2010**, *104*, 93–104.
- (34) Previous studies have shown that both ^{31}P NMR signals of a bisphosphine monoxide ligand shift upfield by $\sim 20\text{--}30$ ppm upon coordination of the phosphine oxide.¹⁴
- (35) Chaplin, A. B.; Scopelliti, R.; Dyson, P. J. *Eur. J. Inorg. Chem.* **2005**, *2005*, 4762–4774.
- (36) Turnover frequencies (TOFs) are calculated by dividing the initial rate of the hydration reaction by the catalyst concentration. Therefore, $\text{TOF} = \text{mol of amide} (\text{mol cat})^{-1} \text{h}^{-1}$.
- (37) Note that deprotonation of PMe_2OH to the corresponding phosphinito ligand PMe_2O^- produces a complex with a more electron donating ligand (the Tolman electronic parameter of PMe_2O^- is 2006 cm^{-1}).³⁸ To probe which of the two species is present during catalysis, titration of 3-Me with sodium hydroxide showed that the P–O–H group has a $\text{p}K_a$ of 4.11 ± 0.08 . For the nitrile hydration reactions done at pH 3.5, the ratio of the acidic to the basic form is thus about 2:1.
- (38) Tolman, C. A. *Chem. Rev.* **1977**, *77*, 313–348.
- (39) Martin, D.; Moraleda, D.; Achard, T.; Giordano, L.; Buono, G. *Chem. Eur. J.* **2011**, *17*, 12729–12740.
- (40) These thermodynamic properties have been observed for the investigation of SN_2 ring-closing reactions of linear α,ω -bromoalkylamines to form cyclic amines and the SN_2 ring-closing reactions of α,ω -bromoalkylcarboxylic acids to form lactones. See: Charton, M. *J. Am. Chem. Soc.* **1975**, *97*, 1552–1556.
- (41) DeTar, D. F.; Luthra, N. P. *J. Am. Chem. Soc.* **1980**, *102*, 4505–4512.
- (42) Knowles, R. R.; Jacobsen, E. N. *Proc. Natl. Acad. Sci. U.S.A.* **2010**, *107*, 20678–20685.
- (43) Charton, M. *J. Am. Chem. Soc.* **1975**, *97*, 1552–1556.
- (44) Previous work has shown that similar complexes of the formula $[\text{Ru}(\eta^6\text{-}p\text{-cymene})\text{Cl}(\text{NCMe})(\text{P}(\text{NMe}_2)_3)]\text{PF}_6$ are chemically and kinetically competent for the hydration of nitriles. See ref 8 and: García-Álvarez, R.; Díez, J.; Crochet, P.; Cadierno, V. *Organometallics* **2011**, *30*, 5442–5451.